International Conference on Space Optics—ICSO 2018

Chania, Greece

9–12 October 2018

Edited by Zoran Sodnik, Nikos Karafolas, and Bruno Cugny

Optical design and modeling of satellite imaging spectrometer for atmosphere monitoring

Yury Dobrolenskiy

Ilya Dziuban

Yuriy Ivanov

Ivan Syniavskyi

et al.

International Conference on Space Optics — ICSO 2018, edited by Zoran Sodnik, Nikos Karafolas, Bruno Cugny, Proc. of SPIE Vol. 11180, 1118065 · © 2018 ESA and CNES · CCC code: 0277-786X/18/$18 · doi: 10.1117/12.2536140

Optical Design and Modeling of Satellite Imaging Spectrometer for Atmosphere Monitoring

Yury Dobrolenskiy*[a], Ilya Dzuban[a], Yuriy Ivanov[b], Ivan Syniavskyi[b], Dmitry Ionov[c], Anatoly Poberovsky[c], Oleg Korablev[a], Anna Fedorova[a], Nikita Vyazovetskiy[a]
[a]Space Research Institute (IKI) of Russian Academy of Sciences, 84/32 Profsoyuznaya str., 117997, Moscow, Russia; [b]Main Astronomical Observatory of National Academy of Sciences of Ukraine, 27 Akademika Zabolotnogo str., 03143, Kyiv, Ukraine; [c]St. Petersburg State University, Faculty of Physics, 7-9 Universitetskaya emb., 199034, St Petersburg, Russia

ABSTRACT

We describe a concept of a satellite imaging spectrometer dedicated for monitoring of the Earth atmosphere operating in the visible and near ultraviolet spectral range. The instrument targets measurements of total ozone as well as other gases (nitrogen dioxide, oxygen and its dimer etc). The instantaneous field of view (IFOV) across track reaches 100° allowing to obtain global daily maps of trace gases content when operating from a typical orbit. The optical concept and design of the instrument, which consists of the entrance unit, two spectrometric channels (for two wavelength ranges) and the calibration unit are described. We also discuss the results of the optical modeling, confirming the proposed characteristics: the spectral resolution of 0.3 nm for the range 300 – 400 nm and 0.5 nm for the range 400 – 800 nm. The angular resolution is ~ 0.5° in both channels that corresponds to ~6×6 km area on the Earth surface for nadir direction from a 700-km orbit.

Keywords: imaging spectrometer, ozone monitoring, space instrument, optical design, UV-visible light

1. INTRODUCTION

Monitoring of total ozone in Earth atmosphere has been provided for decades by measurements at ground-based stations[1] as well as on-board of near-Earth satellites. The latter ones have an advantage of global coverage and, consequently, providing global ozone mapping. Satellite measurements have been performed since 1970s. Among them, one should mention Total Ozone Mapping Spectrometer (TOMS)[2], Global Ozone Monitoring Experiment (GOME and GOME-2)[3-4], Scanning Imaging Absorption Spectrometer for Atmospheric Cartography (SCIAMACHY)[5], Ozone Monitoring Instrument (OMI)[6-7], Ozone Mapping and Profiler Suite (OMPS)[8] et al. Currently, such instruments as OMI (launched in 2004), GOME-2 (launched in 2008) and OMPS (launched in 2011) are operating and providing almost real-time data. A new instrument, TROPOMI (Tropospheric Monitoring Instrument)[9], was launched in October 2017. Start of its operation is planned in 2018.

Similar instruments are also being developed in Russia. Within federal task program “Geophysics”, a piggyback pencil-beam spectrometer was developed to be installed at four ionosphere satellites at near-polar orbits[10]. Qualification prototype of the instrument was manufactured, and a number of ground-based verifications were performed. The total ozone values measured at the ground were close to OMI measurements. As a next step, a new wide-swath imaging spectrometer is now being developed. In the present paper, we describe the optical scheme of this hyper-spectral imager, and confirm its declared parameters by optical modeling.

*dobrolenskiy@iki.rssi.ru; phone 7 495 333-6433; fax 7 495 333-2102; iki.rssi.ru

2. GENERAL DESCRIPTION OF INSTRUMENT

The principal feature of the instrument is its wide IFOV, 100° across track. From an orbit typical for monitoring satellites (700-800 km), such a FOV provides about 2000 km wide swath of observation. This in turn allows for daily global coverage and meets the goal of efficient monitoring of the ozone layer. A similar technique is used by most of current ozone monitoring instruments. For example, total ozone maps from OMI data are made available within several hours after the measurements acquisition (temis.nl).

The instrument includes two spectral channels: the UV channel (300-400 nm) and the VIS channel (400 – 800 nm). The UV channel is supposed to monitor atmospheric ozone O_3 by measurements in the Huggins absorption band (300 – 360 nm). The VIS channel is aimed for measurements of such trace gases as nitrogen dioxide NO_2 at wavelengths 400 – 480 nm, molecular oxygen O_2 near 760 nm, and the oxygen dimer O_4 throughout the range 400 – 600 nm. The both channels are of the same concept and consist of a catadioptric entrance unit (a common entrance unit for the both channels is possible), and a lens spectrometric unit with plane diffraction grating. The detectors are CCD matrixes, registering the spectrum along one axis and the swath along the other. Each swath image consists of 512 pixels across flight direction. For each spatial pixel, the spectrum is measured with 1024 spectral pixels in the UV channel and 2048 spectral pixels in the VIS channel. The spectral resolution is 0.3 nm and 0.5 nm correspondingly. Spatial resolution is about 0.5° for both channels (in both directions), corresponding to pixel size of ~6 km at the surface in nadir direction.

The both spectral channels can be fed by an auxiliary optical entrance for measuring the out-of-atmosphere solar spectra, i.e. to provide sun calibrations. For switching between the observation and calibration modes (nadir survey / sun calibration / dark current calibration), a flipping mirror is planned near the entrance pupil of the instrument, similar to one used in the previous ozonometer[10]. Main characteristics of the instrument are summarized in Table 1.

Table 1: Main characteristics of the instruments.

Parameter	UV channel	VIS channel
Spectral range, nm	300-400	400-800
Spectral resolution, nm	0.3	0.5
FOV (along × across track), degrees	0.5 × 100	0.5 × 100
F-number	F/2	F/3.7
Slit size, mm × mm	19.0 × 0.1	19.0 × 0.1
Diffraction grating		
Type	Plane ruled	Plane ruled
Size, mm × mm	57 × 57	20 × 30
Groove density, mm^{-1}	1650	1200
Reciprocal linear dispersion, nm/mm	8.1	16.3
Detector		
Type	Hamamatsu S10140-1009	Hamamatsu S10140-1109
Number of pixels	1024 × 506	2048 × 506
Pixel size, μm × μm	12 × 12	12 × 12

3. OPTICAL SCHEME OF THE ENTRANCE AND SPECTROMETRIC UNITS

3.1 The entrance unit

The concept of the entrance unit is mainly driven by the requirement of the broad IFOV. Upon analysis of possible lens and mirror designs for the UV-range, a catadioptric (mirror-lens) system was chosen. The scheme of the entrance unit is shown in Fig. 1.

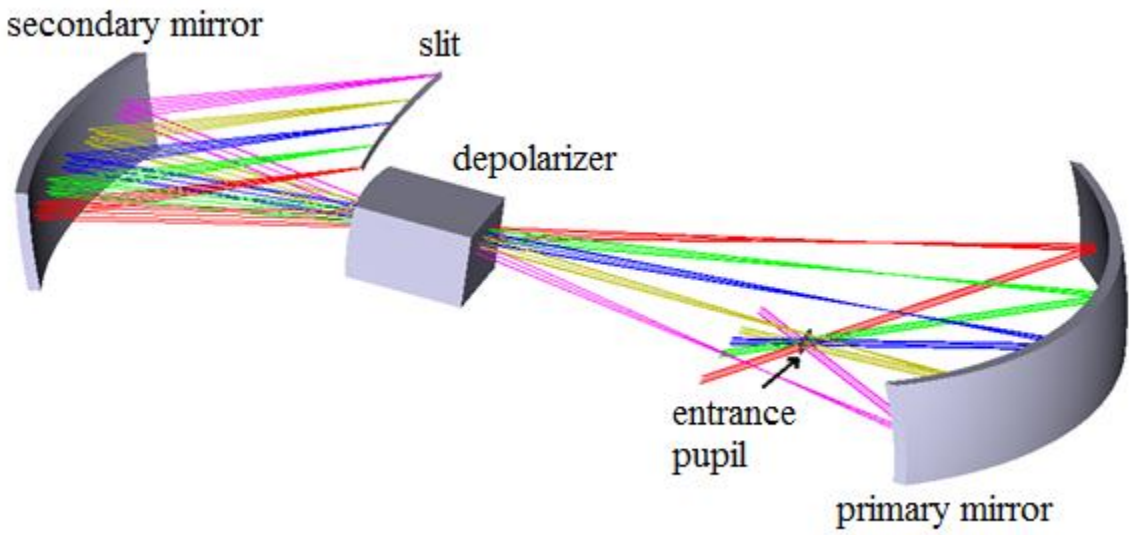

Figure 1. Optical scheme of the entrance unit.

The scheme includes a spherical primary mirror, a scrambler-depolarizer in the pupil and an elliptical secondary mirror illuminating the slit. To simplify the form of the mirror surfaces, a curved slit is utilized. The first surface of quartz depolarizer used for avoiding of polarization effects[7] is made spherical. This helps to correct aberrations in the spectrometric unit. The secondary elliptical mirror has the eccentricity of 0.6.

3.1 The spectrometric unit, UV channel

The optical design of the spectrometric units meets the requirements of spectral and spatial resolution, high transmission and the high aperture ratio. The combination of these requirements led us to avoiding prism schemes as well as schemes based on concave diffraction gratings. The both spectrometric units are designed using the same concept: a spectrometer with a plane diffraction grating, a collimator and a camera objective. The aperture ratio is different in the two spectral channels. The UV channel has F-number of 1:2, and the VIS channel of 1:3.7. The higher aperture ratio compensates for a relatively low light intensity in the UV band, and a lower detector efficiency.

The optical scheme of the UV channel is shown in Fig. 2. Light coming from the slit meets the collimator objective forming a parallel beam. The first lens of the collimator is made of UFS1 colored glass and smoothly attenuates light form 300 to 400 nm in order to equalize the light intensity to a certain extent throughout the range. Other lenses are made of quartz glass, Al_2O_3 and LiF, transparent at wavelengths above 300 nm. The collimated beam incidents on the plane ruled diffraction grating. A standard grating from the Newport catalogue with 1650 grooves/mm was chosen. Light dispersed by the grating passes through a stop diaphragm, positioned right before the camera objective, which focuses the spectrum onto the CCD matrix. We plan to use Hamamatsu S10140-1009 detector with 1024 × 506 pixels (1024 pixels along the spectrum and 506 along the spatial coordinate).

To estimate the instrument performance, we simulated illumination of the entrance pupil with a line spectrum. Fig. 3 shows simulated image at the CCD. There are three groups of lines with wavelengths near 300, 350 and 400 nm. Three lines at each group are separated by 0.3 nm. The slit was assumed 100 μm wide.

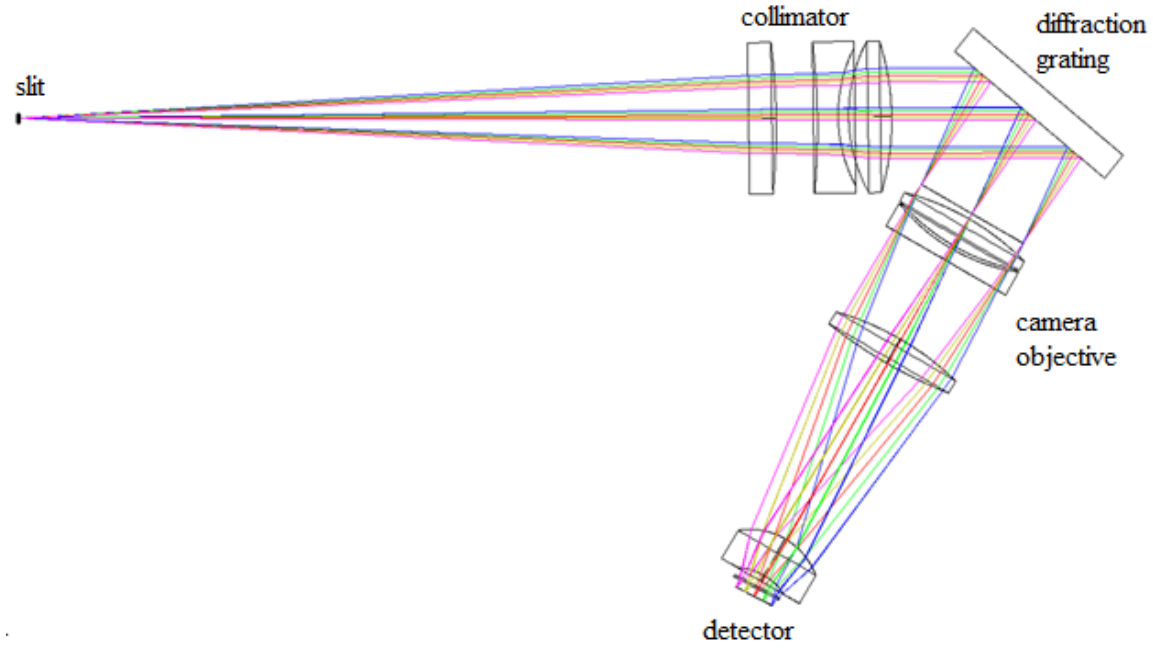

Figure 2. Optical scheme of UV channel.

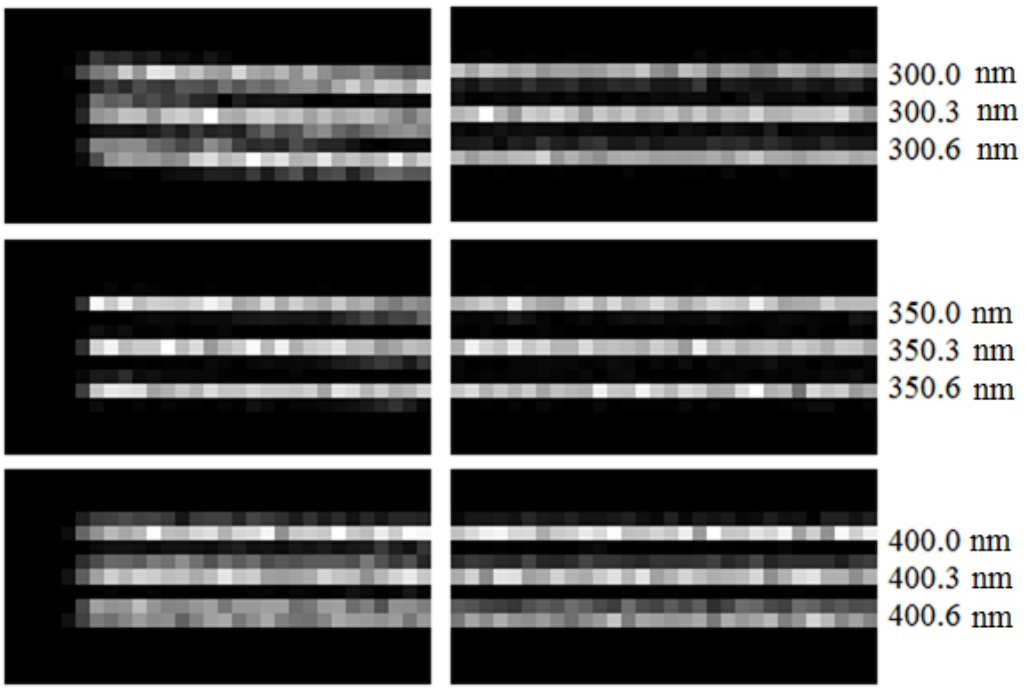

Figure 3. Simulated image of spectral lines on the detector for different wavelengths of UV channel. Left panels show the extremity of the detector, right panels – the central part of the detector.

One can see that in the center of the range (350 nm line group) the lines are clearly separated along the full detector's length. At the edges of the range (300 nm and 400 nm groups), the lines are still well distinguishable in the center with some blurring towards the extremities of the detector, where the curvature of lines introduced by the diffraction grating affects the image. Nevertheless, the resolution of 0.3 nm is achieved throughout the range. Fig. 4 depicts schematically the location of the images shown in Fig. 3 at the detector matrix.

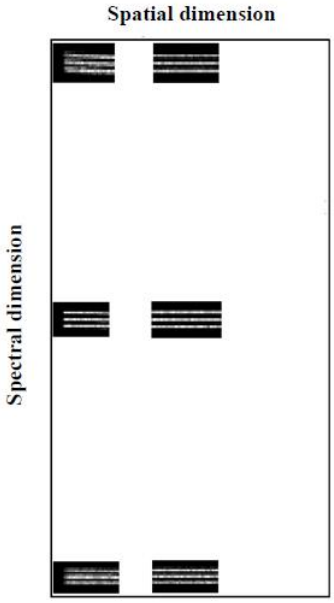

Figure 4. Schematic location of the images shown in Fig. 3 at the detector matrix.

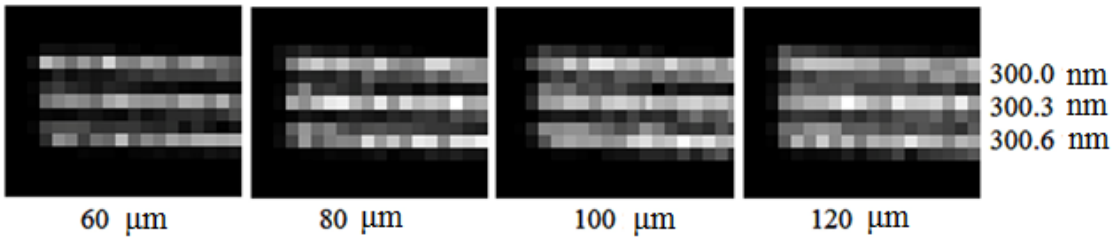

Figure 5. Dependence of spectral lines image on slit width (extremity of the detector).

Fig. 5 illustrates how the same line spectrum depends on the slit width. Clearly, a narrow slit provides better spectral resolution but at the expense of reduced illumination. The maximal slit width for a given spectral resolution would provide the best illumination. In Fig. 5, one can see that the lines are clearly distinguishable up to slit width of about 100 µm. Note that Fig. 5 shows the worst case of Fig. 3 from the point of view of the image quality, at the edge of the spectral range (300 nm), and at the edge of the detector. At the center of the detector and for the center of the spectral range, the image quality is much better. Eventually the slit of 100 µm is chosen as an optimal one for the instrument goals.

3.2 VIS channel

The Optical scheme of the VIS channel is shown in Fig. 6. The ray course is similar to that of the UV channel. A similar Newport plane ruled diffraction grating having a smaller number of grooves is chosen (1200 grooves/mm). The Stop-field diaphragm is also located before the camera objective. As a detector, we plan to use Hamamatsu CCD matrix S10140-1109 with 2048 × 506 pixels (2048 pixels along the spectrum and 506 along spatial coordinate).

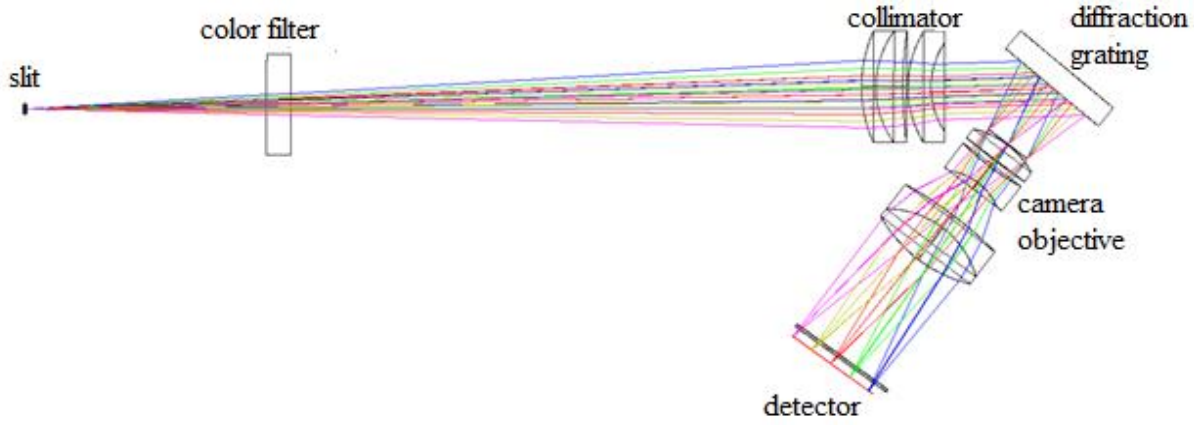

Figure 6. Optical scheme of VIS channel.

The spectral range of this channel is broad, from 400 nm to 800 nm, so there is a risk of diffraction orders overlap, in particular in the red part of spectrum. To block the undesired light, a color filter located prior to the collimator is used. The placement of the filter or its thickness has almost no effect on image quality, so its exact position can be optimized following mechanical constraints.

Fig. 7 depicts a simulated image of the spectral lines on the CCD, similar to that for the UV channel in Fig. 3 and 4. Again, there are three groups of lines with wavelength near 400, 600 and 800 nm separated by 0.5 nm. The 100 μm slit width is assumed. The curvature of the lines is noticeable; one can notice it as the inclination of the lines because Fig. 7 shows only a half of the detector. The spectral resolution as high as 0.5 nm is achieved throughout the range.

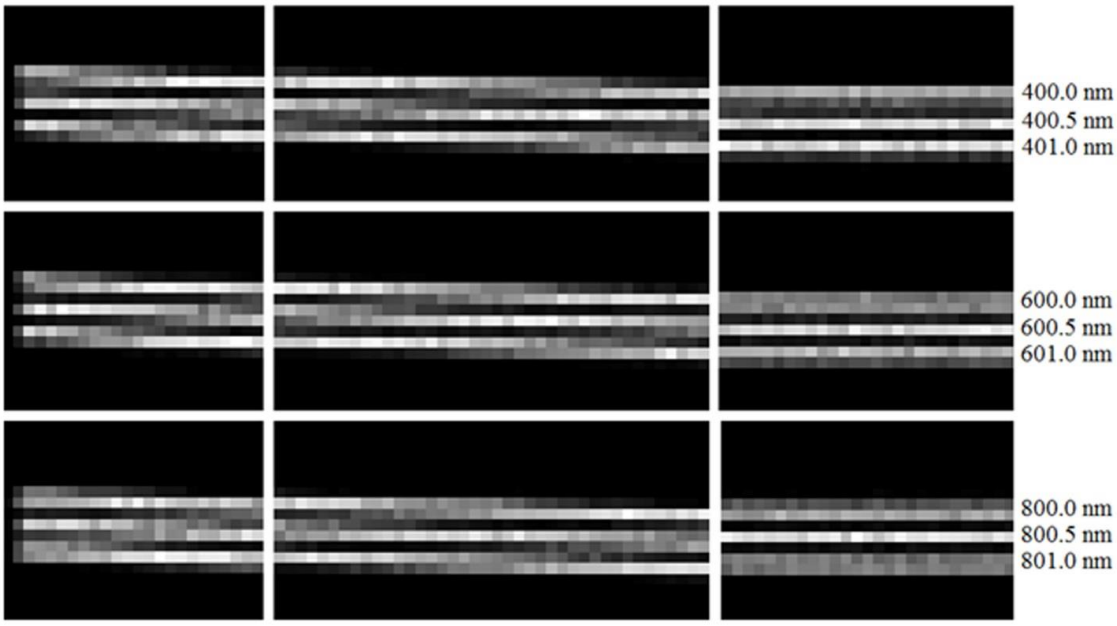

Figure 7. Simulated image of spectral lines on the detector for different wavelengths of VIS channel. The left part corresponds to the extremity of the detector (see Fig. 4), the right part to the center of the detector, the middle part (not considered in Fig. 3 and 4) is the intermediate area in between.

4. CALIBRATION UNIT

As mentioned above, periodical measurements of direct sun spectra are needed to obtain the reference, out-of-atmosphere solar spectrum. For this purpose, an auxiliary optical entrance (or two auxiliary openings, if a different fore-optics will be serving the UV and visible channels) to be pointed towards the sun observations is foreseen. A concept of the calibration unit is shown in Fig. 8. The direct sunlight, considered as a parallel beam reflects from a folding mirror 1, and incidents on a semitransparent mirror 2 used as a beam splitter. Reflected by the splitter, the light goes to the key element of the calibration unit – a diffusing spherical mirror 3, which forms a homogeneous beam, converging at an angle of 100°, corresponding to the instrument's FOV. Then light passes again through the splitter and comes to entrance pupil 4 of the instrument, also shown in Fig. 1.

To switch between the main and the calibration optical entrances, a flipping mirror near the entrance pupil of the instrument is needed. This mirror can also serve as a shutter for dark current calibrations. A specific design of the calibration channel depends on the general layout of the instrument, and on the spacecraft attitude, and shall be optimized accordingly.

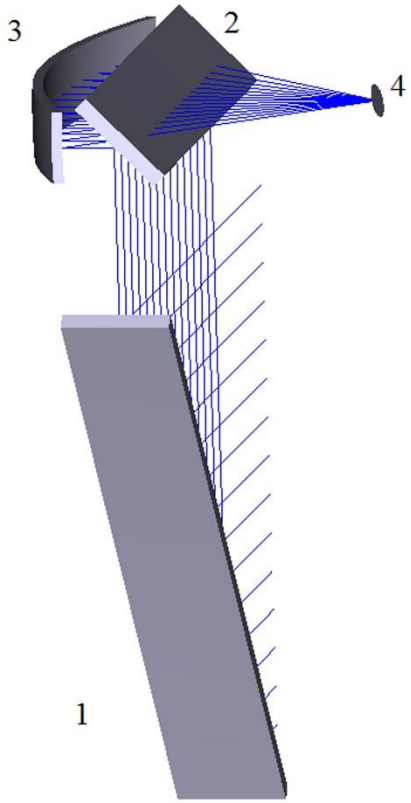

Figure 8. Concept design of the calibration unit. 1 - folding mirror; 2 - semitransparent mirror; 3- diffusing spherical mirror; 4 – entrance pupil of the instrument

5. CONCLUSION

A concept of a wide-swath spectrometer for monitoring of the Earth atmosphere is presented. The instrument is an imaging spectrometer aimed to measure the total ozone content, and other trace gases in the atmosphere. It consists of

two channels: ultraviolet (UV) and visible (VIS), working in near UV and VIS spectral ranges correspondingly. Optical schemes of both channels are developed. The field of view of the spectrometer across track is 100°, the spectral resolution is 0.3 nm in the UV channel, and 0.5 nm in the VIS channel. The F-number is 1:2 for the UV channel, and 1:3.7 for VIS channel. The number of resolvable spectral elements is ≥300 in the UV and ~800 in the VIS channel. We have modeled the instrument performance; in particular, we simulated the image of spectral lines in the detector plane, confirming the declared specifications.

ACKNOWLEDGEMENTS

Yury Dobrolenskiy, Oleg Korablev and Anna Fedorova thank Russian science foundation (RSF Grant16-12-10453) for the support of this research.

REFERENCES

[1] Pommereau, J.-P. and Goutail, F., "O_3 and NO_2 ground-based measurements by visible spectrometry during arctic winter and spring 1988," Geophys. Res. Letters 15, 891-894 (1988).

[2] Heath, D. F., Krueger, A. J., Roeder, H. A. and Henderson, B. D., "The solar backscatter ultraviolet and total ozone mapping spectrometer (SBUV/TOMS) for Nimbus 7," Opt. Eng., 14(4), 323-331 (1975).

[3] Burrows, J. P., Weber, M., Buchwitz, M., Rozanov V. V., Ladstatter-Weissenmayer, A., Richter, A., DeBeek, R., Hoogen, R., Bramstedt, K., Eichmann, K.-U., Eisinger, M. and Perner, D., "The global ozone monitoring experiment (GOME): Mission concept and first scientific results," J. Atmos. Sci. 56, 151–175 (1999).

[4] Munro, R., Lang, R., Klaes, D., Poli, G., Retscher, C., Lindstrot, R., Huckle, R., Lacan, A., Grzegorski, M., Holdak, A., Kokhanovsky, A., Livschitz, J. and Eisinger, M., "The GOME-2 instrument on the Metop series of satellites: instrument design, calibration, and level 1 data processing – an overview," Atmos. Meas. Tech. (9), 1279–1301, (2016).

[5] Bovensmann, H., Burrows, J.-P., Buchwitz, M., Frerick, J., Noel, S., Rozanov, V. V., Chance, K. V. and Goede, A. P. H., "SCIAMACHY: Mission objectives and measurement modes," J. Atmos. Sci., 56(2), 127-150, (1999).

[6] Levelt, P. F., van der Oord, G. H. J., Dobber, M. R., Mälkki, A., Visser, H., de Vries, J., Stammes, P., Lundell, J. O. V. and Saari, H., "The ozone monitoring instrument," IEEE Trans. Geosci. Remote Sens. 44(5), 1093-1101 (2006).

[7] Dobber, M. R., Dirksen, R. J., Levelt, P. F., van der Oord, G. H. J., Voors, R. H. M., Kleipool, Q., Jaross, G., Kowalewski, M., Hilsenrath, E., Leppelmeier, G. W., de Vries, J., Dierssen, W. and Rozemeijere, N. C., "Ozone monitoring instrument calibration," IEEE Trans. Geosci. Remote Sens. 44(5), 1209-1238 (2006).

[8] Kramarova, N. A., Nash, E. R., Newman, P. A., Bhartia, P. K., McPeters, R. D., Rault, D. F., Seftor, C. J., Xu, P. Q. and Labow, G. J., "Measuring the Antarctic ozone hole with the new Ozone Mapping and Profiler Suite (OMPS)," Atmos. Chem. Phys. 14, 2353-2361 (2014).

[9] Veefkind, J. P., Aben, I., McMullan, K., Förster, H., de Vries, J., Otter, G., Claas, J., Eskes, H. J., de Haan, J. F., Kleipool, Q., van Weele, M., Hasekamp, O., Hoogeveen, R., Landgraf, J., Snel, R., Tol, P., Ingmann, P., Voors, R., Kruizinga, B., Vink, R., Visser, H. and Levelt, P. F., "TROPOMI on the ESA Sentinel-5 Precursor: A GMES mission for global observations of the atmospheric composition for climate, air quality and ozone layer applications," Remote Sensing of Environment 120, 70-83 (2012).

[10] Dobrolenskiy, Y. S., Ionov, D. V., Korablev, O. I., Fedorova, A. A., Zherebtsov, E. A., Shatalov, A. E., Mantsevich, S. N., Belyaev, D. A., Vyazovetskiy, N. A., Moiseev, P. P., Tchikov, K. N., Krasavtsev, V. M., Savushkin, A. V., Rumyantsev, D. M., Kananykhin, I. V., Viktorov, A. I., Kozyura, A. V., Moryakin, S. A. and Poberovskii, A. V., "Development of a space-borne spectrometer to monitor atmospheric ozone," Appl. Opt. 54(11), 3315-3322 (2015).